EFFECT OF MUSCLE CONTRACTION IN HIGH SPEED CAR-PEDESTRIAN IMPACT – SIMULATIONS FOR WALKING POSTURE

Soni A., Chawla A., Mukherjee S.

Department of Mechanical Engineering, Indian Institute of Technology, New Delhi, INDIA

Malhotra R.

Department of Orthopaedics, All India Institute of Medical Sciences, New Delhi. INDIA

ABSTRACT

This paper investigates the effect of muscle contraction on lower extremity injuries for pedestrian walking posture in car-pedestrian lateral impact at 40 kmph. The full body model, PMALE, which was configured in symmetric standing posture, has been repositioned in the walking posture. Finite element simulations have then been performed using the PMALE in the walking posture and front structures of a car. Two impact configurations, i.e. impact on right (trailing) and on left (leading) leg have been simulated. Two pre-impact conditions, that of a symmetrically standing pedestrian, representing a cadaver and an unaware pedestrian have been simulated for both the impact configurations. Stretch based reflexive action was included in the simulations for an unaware pedestrian. It is concluded that (1) with muscle contraction risk of ligament failure decreases (2) in lateral impacts, MCL could be considered as the most vulnerable and LCL as the safest ligament (3) for a walking pedestrian, PCL would be at higher risk in case of impact on trailing leg whereas, ACL would be at higher risk if car strikes the leading leg (4) active muscles may not affect bone fracture in high speed car-pedestrian crashes.

Keywords: PMALE, Lower extremity model, Finite element model, Dynamic simulation, Muscle contraction, Standing posture, Walking posture, Car-pedestrian impact, Knee injury

PEDESTRIANS CONSTITUTE 65% of the 1.17 million people killed annually in road traffic accidents worldwide (World Bank 2001). Epidemiological studies on pedestrian victims have indicated that together with the head, lower extremities are the most frequently injured body region (Chidester et al. 2001; Mizuno 2003). Pedestrian Crash Data Study (PCDS) (Chidester et al. 2001) reports that passenger cars have the biggest share in vehicle-pedestrian accidents. Further, the front bumper was the major source of injury to the lower extremity when injuries were caused by a vehicle structure (Mizuno 2003). This has posed a challenge for vehicle designers to design pedestrian friendly car front structures. To devise effective pedestrian protection systems, it is essential to understand the injury mechanism.

So far, lower limb injury mechanism in car-pedestrian crashes has been studied through tests on human cadaver specimens (Kajzer et al. 1990, 1993, 1997, 1999; Bhalla et al. 2005) and simulations using validated passive finite element (FE) models (Schuster et al. 2000; Maeno et al. 2001; Takahashi et al. 2001; Nagasaka et al. 2003; Chawla et al. 2004; Soni et al. 2007). However, the major shortcoming in these existing experimental and computational studies is that they do not account for muscle action. Therefore, effects of pre-crash muscle contraction on the response of lower limbs in car-pedestrian crashes remained unclear.

Of late, Soni et al. (2007) have investigated the probable outcome of muscle contraction using a lower limb (single leg) FE model with active muscles (A-LEMS). More recently, Soni et al. (2008) have extended the single leg model A-LEMS to a full body Pedestrian Model with Active Lower Extremities (PMALE) and studied the effects of muscle contraction on the response of lower extremity for a symmetrically standing pedestrian (with legs in side by side stance) in full scale car-pedestrian impact. However, Pedestrian Crash Data Study (PCDS) (Chidester et al. 2001) reported that prior to the crash, only 4% pedestrian were in the stationary standing posture whereas, 55%, were walking.

The present study extends our earlier studies to investigate the effect of muscle contraction on the response of lower limb for pedestrian walking posture in full scale car-pedestrian lateral impact at high speed. The PMALE, which was configured in standing posture, has been repositioned in the walking posture. The real world car-pedestrian lateral impact has then been simulated using the PMALE configured in the walking posture (PMALE-WP) and front structures of a validated car FE model. Two impact configurations, i.e. impact on the right leg and the left leg of PMALE-WP, have been simulated. Two sets of simulations, i.e. with deactivated muscles and with activated muscles (including reflex action) mimicking an unaware walking pedestrian have been performed for both the impact configurations. Knee kinematics, strains in knee ligaments and VonMises stresses in bones for two levels of muscle activation have then been compared to assess the effect of muscle contraction.

METHODS

PMALE IN WALKING POSTURE

Here, PMALE, which was configured in symmetrically standing posture of a pedestrian with legs in side by side stance, has been repositioned in the walking posture. Relative angles, amongst the body segments, required to define alignment of the walking posture (Figure 1) are taken from Mizuno et al. (2003).

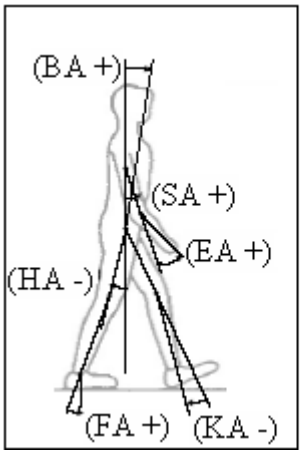

BA: Back Angle
HA: Hip Angle
EA: Elbow Angle
FA: Foot Angle
KA: Knee Angle
SA: Shoulder Angle

	Definition Angle (deg)	
	Left Leg	Right Leg
BA	+ 5	
SA	- 15	+ 15
EA	0	+ 27
HA	+ 29	- 12
KA	- 14	- 10
FA	0	+ 22

Figure 1 Definition of walking posture taken from Mizuno et al. (2003)

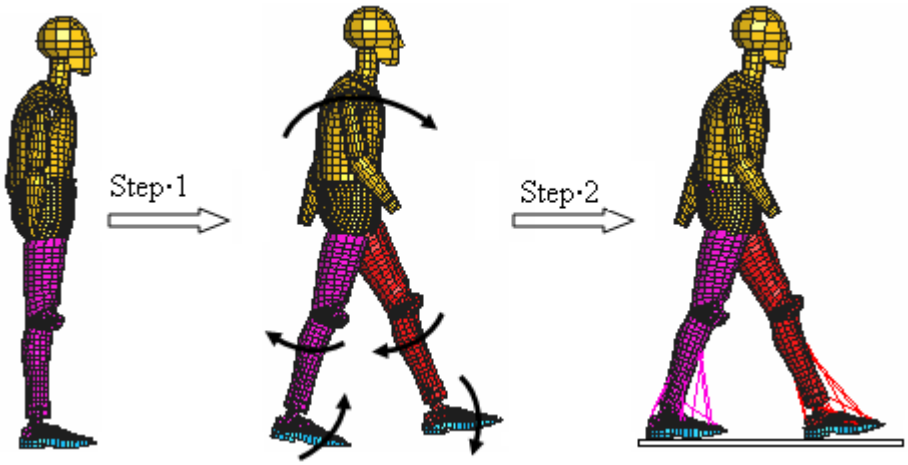

Figure 2 Repositioning the PMALE from symmetric standing posture to walking posture

Series of FE simulations of short duration have then been performed with the PMALE (configured in the standing posture) to reposition its body segments in the walking posture. Figure 2 illustrates the major intermediate stages of the model repositioning from symmetric standing posture to walking posture (referred as PMALE-WP). In PMALE-WP, left leg is leading to the right leg such that the left leg (i.e. leading leg) corresponds to the heel strike phase (i.e. left heel is just landed on the ground) of the human gait cycle whereas, the right leg (i.e. trailing leg) corresponds to the terminal

stance phase (i.e. right heel is about to leave the ground). Upper body is leaned forward by 5 degrees with the vertical axis passing though the attachment location of upper body with the top of sacrum.

SIMULATION SETUP

Simulations have then been done with the PMALE-WP and front structures of a validated car FE model to reproduce the real world car-pedestrian crashes. Figure 3 shows the setup of these simulations.

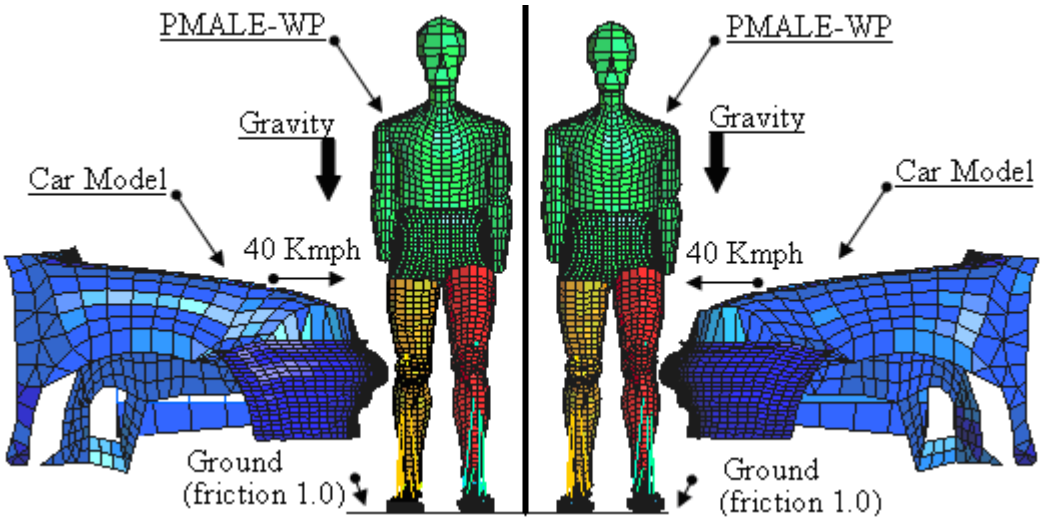

(a) (b)

Figure 3 Simulation set up used in the present study for (a) impact on right leg and (b) impact on left leg

Here, PMALE-WP represents a pedestrian walking on rigid ground in a gravity field. The coefficient of friction between shoe and ground is set to 1.0 as suggested for grooved rubber on road (Li K.W. et al. 2006). Car model with a total mass of 1158 kg (mass of the front structures is 355 kg and 803 kg is modeled as added mass to account for the remaining car structures) is propelled towards the PMALE-WP with an impact speed of 40 kmph. Since, in real world car-pedestrian crashes, a car may approach a pedestrian from its right or left side. Thus, impact on lateral side of the right leg (Figure 3 (a)) and the left leg (Figure 3 (b)) have been simulated. The PMALE-WP is placed in front of the car model such that it interacts with mid portion of the bumper whereas; the car model is positioned at a height above the ground such that it corresponds to the car rolling on its tyres.

PEDESTRIAN PRE-IMPACT CONDITIONS

Two pre-impact pedestrian conditions, i.e., one with deactivated muscles (cadaveric) and the other with activated muscles (including reflex action) for an unaware pedestrian have been simulated for both the impact configurations in the present study. We call these conditions cadaveric and reflex conditions respectively. These conditions differ in terms of initial activation levels in muscles and whether the reflex action is enabled. By enabling the reflex action for a muscle, the activation level in that muscle rises with time during the simulation; thereby increasing the force produced by that muscle.

Cadaveric Condition: In this condition, a cadaver aligned in walking posture has been simulated. To model a cadaver in FE simulation, all the muscles in PMALE-WP have been assigned the minimum value of 0.005 as the initial activation level. The reflex action is disabled. As a result, in this condition, activation levels in each muscle remain at the minimum value (i.e. 0.005) for the entire duration of the simulation. Therefore, all the muscles function at their minimum capacity.

Reflex Condition: In this condition, a pedestrian who is walking on road and is unaware of an impending crash has been simulated. Here, we have considered that prior to the impact, pedestrian's right leg (i.e. trailing leg) is in terminal stance phase (i.e. right heel is about to leave the ground) of the human gait cycle and left leg (i.e. leading leg) is in heel strike phase (i.e. left heel is just landed on the

ground). To model an unaware pedestrian in such walking posture, right leg muscles have been assigned the activation levels corresponding to the terminal stance i.e. 60% gait whereas, muscles in the left leg have been assigned the activation levels corresponding to heel strike i.e. 0% gait. Values of these muscle activation levels (Table A1 in Appendix A) have been taken from the electromyography (EMG) levels recorded in human subjects during the gait cycle by Winter (1987).

A stretch based involuntary reflex action has also been enabled in this condition. For enabling the reflex, a threshold value of elongation is to be defined in Hill material card of a muscle. When the elongation in muscle crosses the threshold value, stretch reflex in a muscle gets activated. However, the increase in muscle force starts only after a certain time known as reflex time. This delay between the activation of stretch reflex and the onset of increase in muscle force represents the time taken by the signal to travel through the central nervous system (CNS) circuitry (muscle-spinal cord-muscle). A delay of 20 ms has been assigned to all the muscles in PMALE-WP (Ackerman 2002). This mimics the ability of live muscle to respond to a small stretch produced by an outside agency. In medical terms, this kind of reflex action is known as “stretch reflex” (Vander et al. 1981).

DATA ANALYSIS

Two nodes at both femur and tibia have been selected to obtain the nodal time history in simulations. Relative movements of selected nodes are then used to calculate relative tibia displacements and knee joint angles. Sign conventions used here are as per the SAE standards. Element elimination approach has been enabled to simulate the failure in the ligaments and bones. Knee kinematics, strain time history of each knee ligament and VonMises stress contours in bones of the impacted leg of PMALE-WP have been recorded from the simulations. Response in cadaveric and reflex conditions has then been compared to determine the role of muscle contraction.

RESULTS AND DISCUSSION

In all, four simulations, each of 100 ms duration, have been performed in the present study. For the first 50 ms (stabilization duration), PMALE-WP has been stabilized under gravity load in each simulation. At the end of first 50 ms, car front impacts the right leg or the left leg of the stabilized PMALE-WP. Knee kinematics, ligament strains and VonMises stresses in bones have been recorded from the simulations to assess the effect of muscle contraction. Results presented here are for the impact duration and the initial time (i.e. 0 ms) corresponds to the time of contact.

RIGHT LEG IMPACT CONFIGURATION

In this section, we present the results obtained from the simulations of impact on the right leg in both cadaveric and reflex conditions.

Knee Joint Kinematics

Linear and angular tibia displacement time histories relative to femur for both cadaveric and reflex conditions are compared in Figure 4 and Figure 5, respectively. It is evident that active muscle forces have significantly affected the knee joint kinematics in reflex condition as compared to the cadaveric condition.

In simulations for both cadaveric and reflex conditions, it has been observed that the car front impacts on the knee joint of the right leg in the lateral side. As a result, both tibia and femur at the knee level are forced to move in the medial direction. Due to this, relative medial tibia displacement (Figure 4 (a)), inferior (i.e. away from femur) tibia displacement (Figure 4 (c)) and medial knee bending angle (Figure 5 (b)) increases in the initial 20 ms.

After 20 ms, momentum of the car front further pushes the tibia and the femur at the right knee joint to move together in the medial direction. Since, the right leg is rigidly attached to the massive upper body via the pelvis at the femur end, this event further increases the medial knee bending angle (Figure 5 (b)) and the inferior tibia displacement (Figure 4 (c)), whereas, the relative medial tibia displacement (Figure 4 (a)) remains nearly constant till 28-30 ms. About 28-30 ms, the lower leg moves in the posterior direction and eventually increases the posterior tibia displacement (Figure 4 (a)) and the knee flexion (Figure 5 (a)).

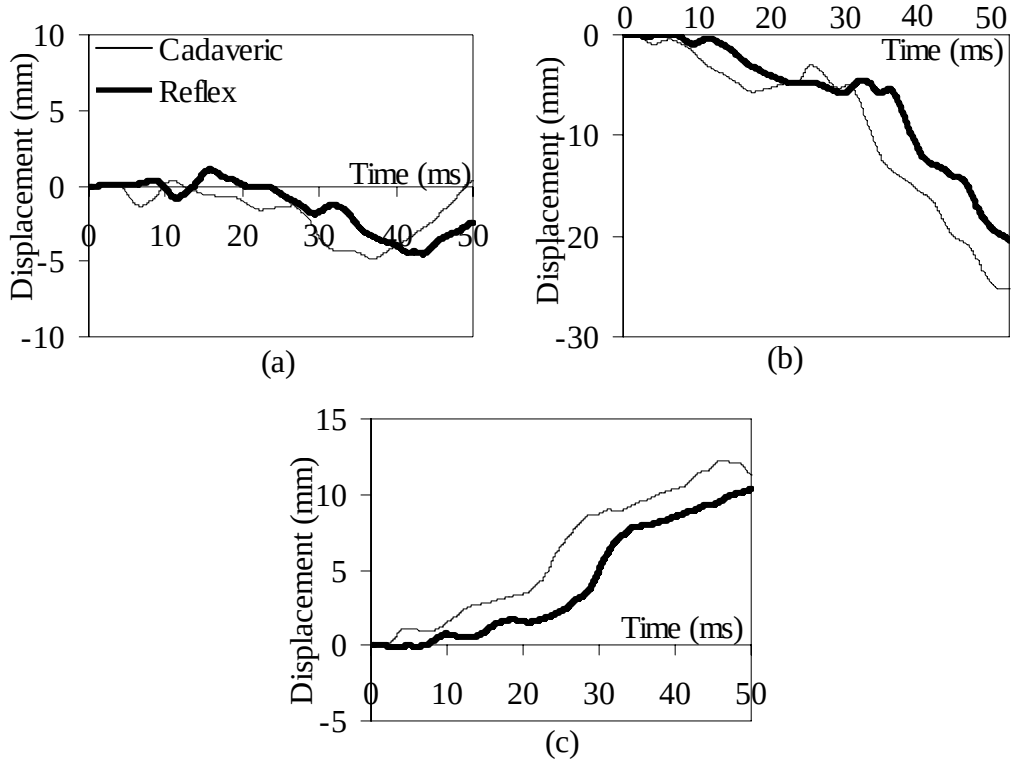

Figure 4 Comparison of relative tibia displacements of the impacted leg (i.e. right leg) in (a) anterior-posterior (b) lateral-medial and (c) inferior-superior directions

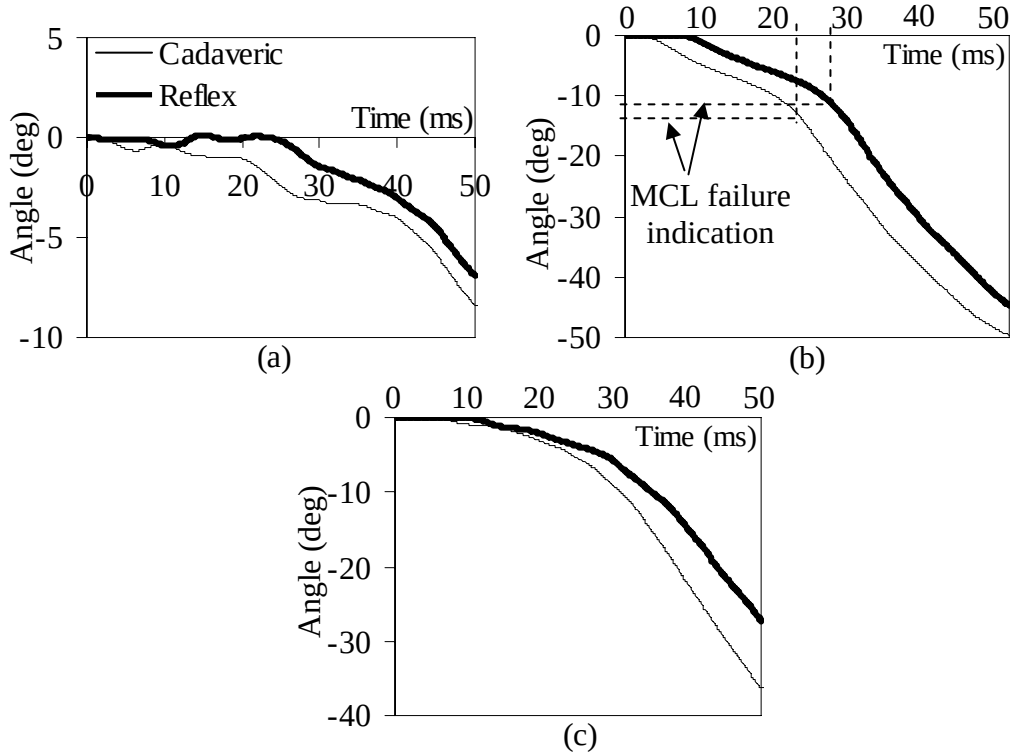

Figure 5 Comparison of relative knee angles of the impacted leg (i.e. right leg) (a) extension-flexion (b) medial-lateral bending and (c) internal-external rotations

Then, about 29-33 ms, the right foot leaves the ground and by the same time right tibia shaft fractures. Due to this, the right leg also comes into motion and then rotates the pelvis. As the pelvis is rigidly connected to the upper body at sacrum; this event eventually sets the medial rotation (i.e.

towards car bonnet) in the upper body. Effect of these events is noticeable as a sudden rise in the medial tibia displacement (Figure 4 (a)) and all three knee angles in Figure 5, i.e., the knee flexion, the medial knee bending angle and the knee external rotation.

In the reflex condition, active muscle forces pull the tibia towards the femur. As a result, all the relative tibia displacements (Figure 4) and knee angles (Figure 5) remained consistently lower in the reflex condition as compared to the cadaveric condition.

Strain in Knee Ligaments

Figure 6 illustrates the calculated strain time history in the knee ligaments of the right leg of PMALE-WP for both cadaveric and reflex conditions. It is evident that strains in knee ligaments have reduced significantly in the reflex conditions as compared to the cadaveric condition.

ACL: Figure 6 (a) compares the strain time history in ACL for both the conditions. It is observed that till 22 ms and 28 ms, ACL remained nearly unstrained, in the cadaveric and the reflex conditions, respectively. After that, strain in ACL reached the peak values of 2.93% (cadaveric) and 2.35% (reflex) within 5-6 milliseconds. The sudden rise in ACL strain in both the conditions can be related with MCL failure (Figure 6 (c)) which suggests that after MCL failure, the load gets transferred to the ACL. Later, for the remaining portion of the simulations, ACL strain remained nearly constant in both the conditions. This can be attributed to fracture in tibia shaft which has prevented the ACL strain to increase further.

It is observed that, in the reflex condition peak strain in ACL has dropped by a factor of 1.25 as compared to the cadaveric condition. This can be attributed to the combined effects of reduced inferior tibia displacement (Figure 4 (c)), knee flexion (Figure 5 (a)) and medial knee bending (Figure 5 (b)) in the reflex condition than in the cadaveric condition.

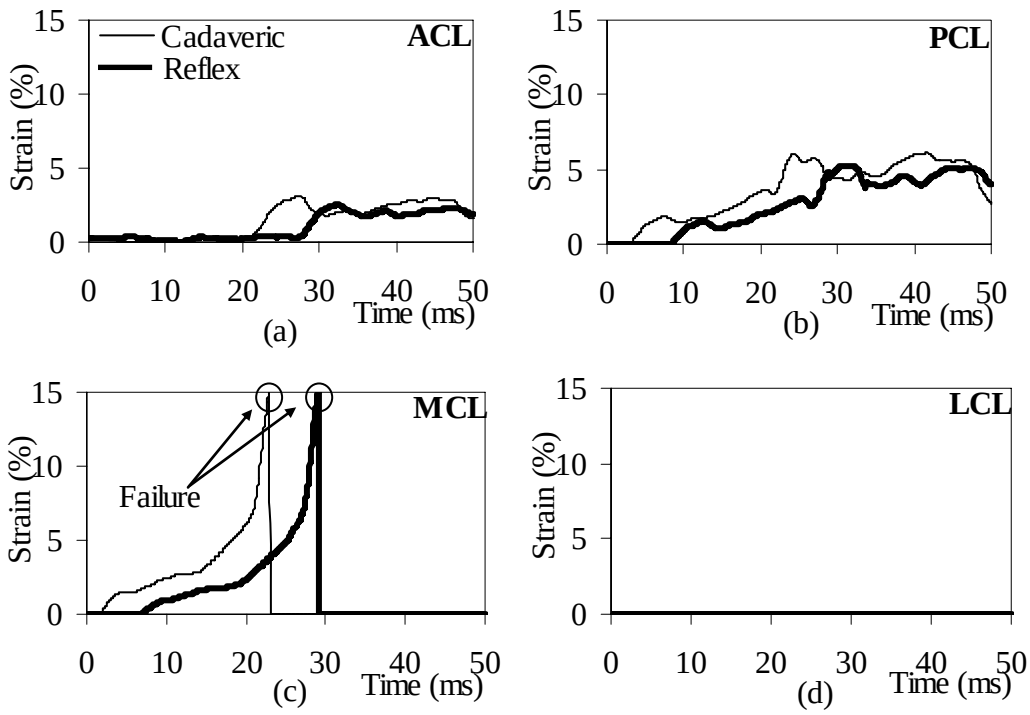

Figure 6 Comparison of strain time history in knee ligaments (a) ACL (b) PCL (c) MCL and (d) LCL of the right leg

PCL: Strain time history in PCL is compared for both the conditions in Figure 6 (b). It is apparent that reduction in strain due to muscle action is more prominent in PCL than in the ACL. About 25-30 ms, a sudden jump in PCL strain has been observed in both the conditions which can be related with MCL failure (Figure 6 (c)). After that, PCL strain remained nearly constant for the

remaining portion of the simulations in both the conditions. This can be attributed to fracture in tibia shaft which has relieved the PCL.

In the reflex condition, peak strain value in PCL has dropped by a factor of 1.21 as compared to the cadaveric condition. Relative displacement of tibia in the inferior direction is the major source of strain in the PCL. Figure 4 (c) illustrates that in both cadaveric and reflex conditions, the tibia is moving away from the femur. However, active muscle forces in the reflex condition have pulled the tibia towards the femur and therefore; tibia displacement in inferior direction (away from the femur) has reduced (Figure 4 (c)). This has slackened the PCL in the reflex condition.

MCL: MCL strain for both the conditions is shown in Figure 6 (c). It is observed that peak MCL strain has reached the ligament failure limit of 15% in both the conditions. However, in comparison to the cadaveric condition, failure is delayed by 6.2 ms in the reflex condition (23 ms to 29.2 ms). The delay in MCL failure can be attributed to the combined effect of reduced inferior tibia displacement (Figure 4 (c)) and medial knee bending (Figure 5 (b)) in the reflex condition as compared to the cadaveric condition. Rupture in MCL in both the simulations agrees with the results of statistical analysis of real world accidents in which MCL is reported as the most frequently injured knee ligament (Matsui 2001).

LCL: It is observed the LCL (Figure 6 (d)) has remained unstrained in both the conditions. This can be ascribed to the lateral impact which forces tibia to bend medially and consequently keeps the LCL slackened.

VonMises Stresses in Bones

Figure 7 compares the VonMises stress distribution on the bones (i.e. femur, tibia and fibula) of the right leg in both cadaveric and reflex condition. It is observed that, in both cadaveric and reflex conditions stresses in the medial side of mid tibia and mid fibula regions have reached their ultimate stress limits and hence fractured in the simulations. However, in the reflex condition fracture in medial side of the mid tibia has delayed by 4 ms as compared to the cadaveric condition (29.2 ms as against 33.2 ms).

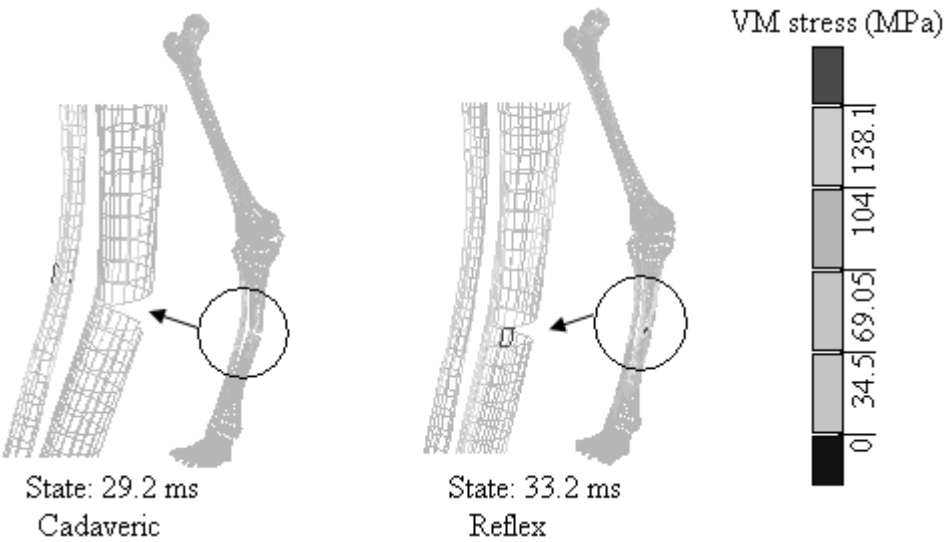

Figure 7 Comparison of VonMises stress distribution in bones of the right leg in both cadaveric and reflex conditions

LEFT LEG IMPACT CONFIGURATION

This section presents the results obtained from the simulations of impact on the left leg in the cadaveric and reflex conditions.

Knee Joint Kinematics

Linear and angular tibia displacements relative to femur for both cadaveric and reflex conditions are compared in Figure 8 and Figure 9, respectively. It is evident that active muscle forces have significantly affected the knee joint kinematics in reflex condition as compared to the cadaveric condition.

In simulations for both cadaveric and reflex conditions, it has been observed that the car front impacts on the knee joint of the left leg in the lateral side. As a result, both tibia and femur at the knee level are forced to move in the medial direction. Due to this, relative medial tibia displacement (Figure 8 (a)) and medial knee bending angle (Figure 9 (b)) increase consistently during the entire duration of both the simulations.

At about 29-33 ms, left foot leaves the ground and by the same time left tibia shaft fractures. This eventually sets motion in the left leg. Since, the left leg is rigidly attached to the massive upper body via the pelvis at the femur end and is in forward stance, inertia of the moving lower leg suddenly increases the anterior tibia displacement (Figure 8 (a)) and the knee extension (Figure 9 (a)).

It is apparent from Figure 8 and Figure 9 that in the left leg impact configuration, the medial tibia displacement and the medial knee bending have remained consistently higher than other knee kinematics parameters in both cadaveric and the reflex conditions. However, in the reflex condition, active muscle forces has pulled tibia close to the femur and therefore significantly reduced the relative linear and angular tibia displacements in all the directions.

It is interesting to note that, in the reflex condition tibia has moved in the superior direction (i.e. towards femur) (Figure 8 (c)) whereas it has moved in the inferior direction (i.e. away from the femur) in the cadaveric condition. This is due to the higher active muscle forces in the reflex condition which has pulled tibia towards the femur.

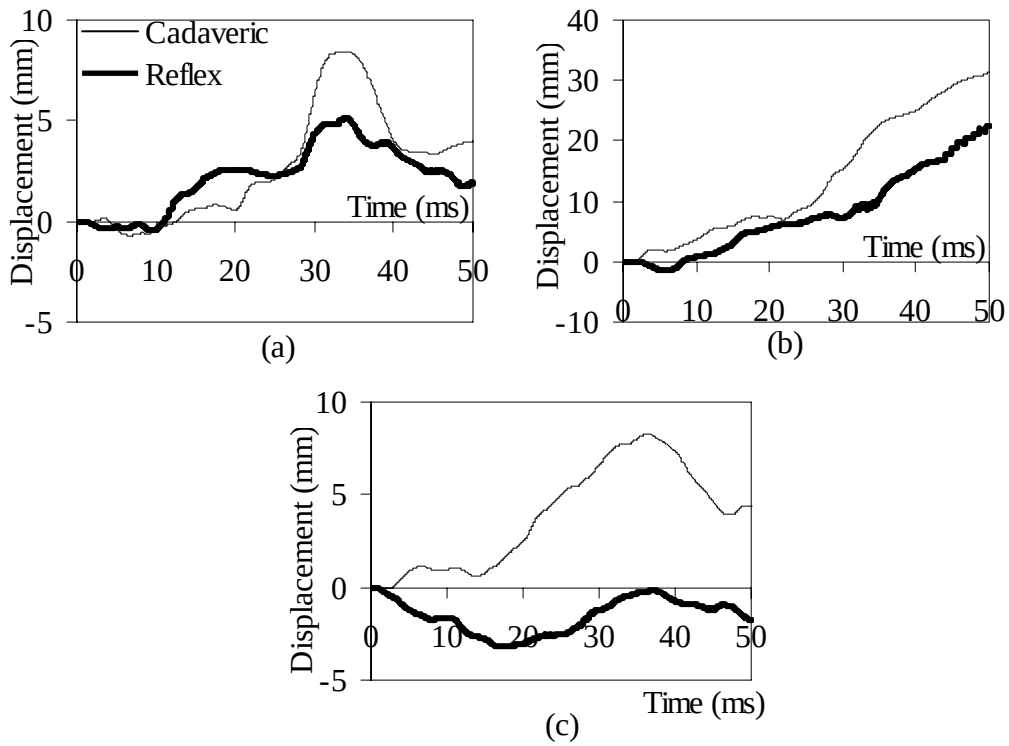

Figure 8 Comparison of relative tibia displacements of the impacted leg (i.e. left leg) in (a) anterior-posterior (b) medial-lateral and (c) inferior-superior directions

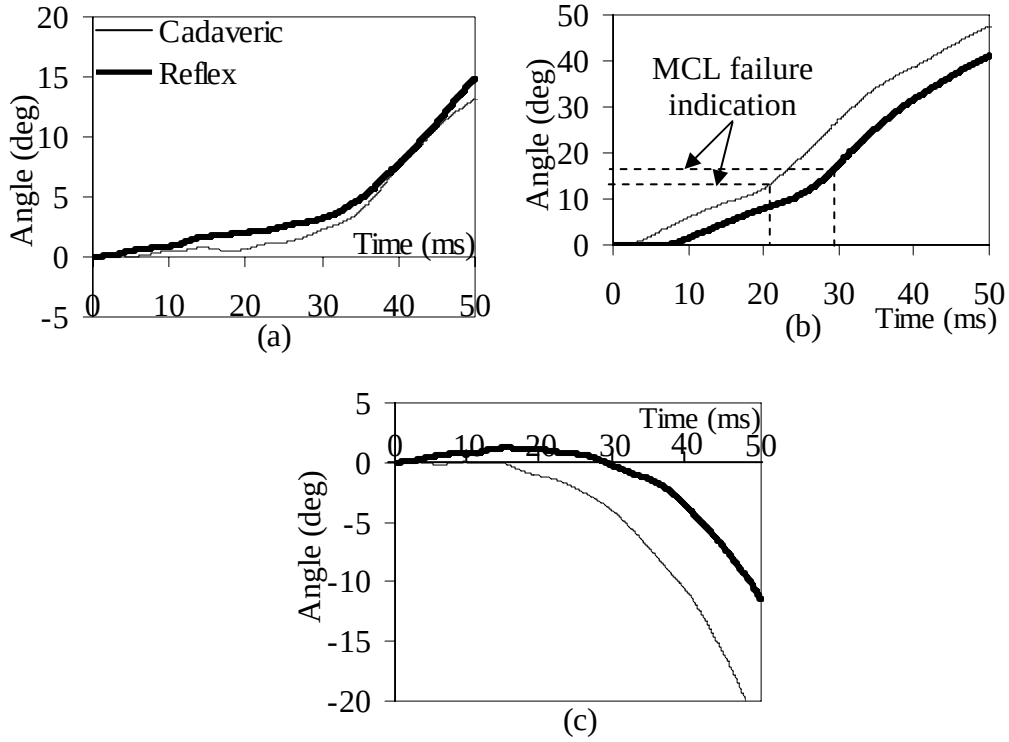

Figure 9 Comparison of relative knee angles of the impacted leg (i.e. left leg) (a) extension-flexion (b) medial-lateral bending and (c) internal-external rotations

Strain in Knee Ligaments

Figure 10 illustrates the strain time history in knee ligaments of the left leg of PMALE-WP for both cadaveric and reflex conditions. It is evident that strains in knee ligaments have reduced significantly in the reflex conditions as compared to the cadaveric condition.

ACL: Figure 10 (a) compares the strain time history in ACL for both the conditions. It is observed that in the cadaveric condition, peak ACL strain has reached the ligament failure limit of 15% at 27.9 ms. Whereas, in the reflex condition; strain in ACL remained nearly 0% till 10 ms and gradually increased to 2.88% at around 28 ms. The ACL strain has then risen to 6% at about 32 ms which could be related to failure in MCL in the reflex condition (Figure 10 (c)). Immediately after this, i.e. at about 33.2 ms, tibia fracture occurred due to which ACL strain dropped to 5% and remained nearly constant for the remaining portion of the simulation.

PCL: Strain time history in PCL is compared for both the conditions in Figure 10 (b). It is observed that, in the reflex condition strain in PCL has remained lower than the cadaveric condition for the entire duration of the simulation. It is found that peak strain in PCL has dropped by a factor of 2.07 in the reflex condition (3.2%) as compared to the cadaveric condition (6.63%). Relative displacement of tibia in the inferior direction is the major source of strain in the PCL. Figure 8 (c) illustrates that in the cadaveric condition tibia is moving away from the femur (i.e. in the inferior direction) whereas, in the reflex condition active muscle forces have pulled the tibia towards the femur (i.e. in the superior direction). This has slackened the PCL in the reflex condition.

MCL: MCL strain for both the conditions is shown in Figure 10 (c). It is observed that peak MCL strain has reached the ligament failure limit of 15% in both the conditions. However, in comparison to the cadaveric condition, failure is delayed by 9 ms in the reflex condition (29.90 ms as against 20.90 ms). The delay in MCL failure can be attributed to the reduced medial knee bending (Figure 9 (b)) in the reflex condition as compared to the cadaveric condition.

LCL: It is observed that strain in LCL (Figure 10 (d)) has remained unstrained in both the conditions. This can be ascribed to the lateral impact which forces tibia to bend medially and consequently keeps the LCL slackened.

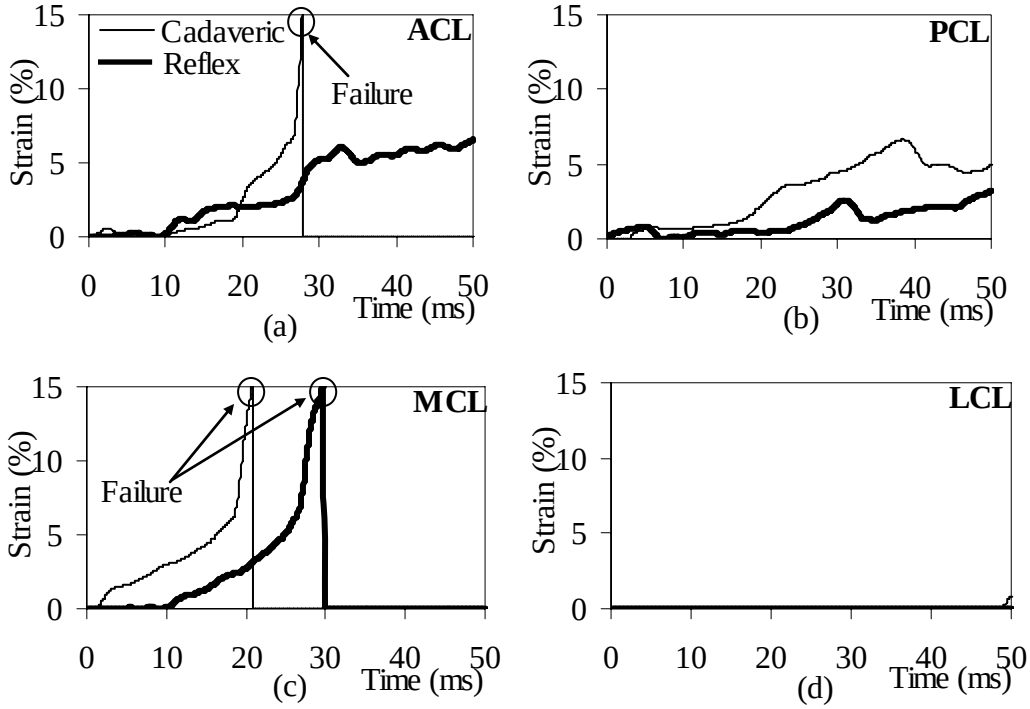

Figure 10 Comparison of strain time history in knee ligaments (a) ACL (b) PCL (c) MCL and (d) LCL of the left leg

VonMises Stresses in Bones

Figure 11 compares the VonMises stress distribution on the bones (i.e. femur, tibia and fibula) of the left leg in both cadaveric and reflex condition. It is found that tibia has fractured in both the conditions. However, tibia fracture has delayed by 4 ms in the reflex condition (33.2 ms) as compared to the cadaveric condition (29.2 ms).

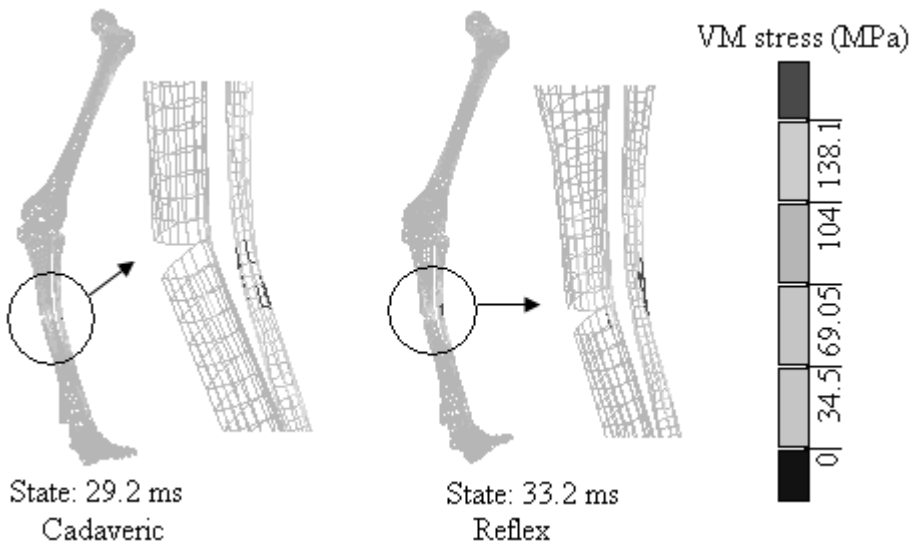

Figure 11 Comparison of VonMises stress distribution in bones of the left leg in both cadaveric and reflex conditions

CONCLUSIONS

In the present study, effect of muscle contraction on the response of lower limb in high speed lateral impact was studied for the pedestrian walking posture. The full body model with active lower extremities i.e. PMALE, was repositioned from standing posture to the walking posture. Real world

car-pedestrian lateral impacts were simulated using the PMALE-WP and front structures of a validated car FE model. Two impact configurations, i.e. impact on the right leg and on the left leg were simulated. For each impact configuration, two sets of simulations, i.e. one with deactivated muscles (cadaveric condition) and the other with activated muscles (including reflex action) mimicking an unaware walking pedestrian were performed. Differences in responses of a cadaver and an unaware pedestrian were then studied. To assess the effect of muscle activation, strains in knee ligaments and VonMises stresses in bones were compared. We conclude that:

1. In both the impact configurations, peak strains in the knee ligaments were lower in the reflex condition (with active muscles) as compared to the cadaveric condition. This supports our previous findings that the risk of ligament failure in real life crashes is likely to be lower than that predicted through cadaver tests or simulations.
2. It was found that; strain in ACL was higher than PCL strain in case of impact on the leg in heel strike phase (i.e. the leading leg). Whereas, in case of impact on the leg in the terminal stance phase (i.e. the trailing leg), this pattern of higher strain reversed, means, strain in PCL was higher than ACL strain. This leads to the conclusion that knee ligament failure is posture specific.
3. In all the four simulations, MCL has failed, whereas, LCL remained nearly unstrained. This implies that in lateral impacts, MCL could be considered as the most vulnerable and LCL as the safest ligament.
4. In all the four simulations, tibia and fibula were fractured. This suggests that active muscles may not have significant effect on bone fracture in high speed car-pedestrian crashes.
5. It is observed that bone fracture unloads the knee joint and hence reduces the chances of ligament failure.

It must however be noted that the muscle parameters used in the present study represent an average male. Muscle strength (maximum force capacity combining fatigue level) varies from one individual to another and also with age and gender. However, these effects are not quantified and studies need to be conducted to quantify the effect of these parameters.

ACKNOWELEDEGEMENT

The authors would like to acknowledge the support from the Transportation Research and Injury Prevention Program (TRIPP) at Indian Institute of Technology Delhi and the Volvo Research Education Foundation.

REFERENCES

1. Bhalla, K., Takahashi, Y., Shin, J., Kam, C., Murphy, D., Drinkwater, C., and Crandall, J., Experimental investigation of the response of the human lower limb to the pedestrian impact loading environment, In Proceedings of the Society of Automotive Engineer World Congress 2005, SAE Paper 2005-01-1877.
2. Chawla, A., Mukherjee, S., Mohan, D., and Parihar, A., Validation of lower extremity model in THUMS, In Proceedings of the IRCOBI 2004, pp. 155-166.
3. Chawla, A., Mukherjee, S., Soni, A., and Malhotra, R., Effect of active muscle forces on knee injury risks for pedestrian standing posture at low speed impacts, In Proceedings of the IRCOBI conference, pp. 95-112, 2007.
4. Chidester, A. B., and Isenberg, R. A., Final report - the pedestrian crash data study, In Proceedings of the 17th ESV conference 2001.
5. Kajzer, J., Cavallero, S., Ghanouchi, S., and Bonnoit, J., Response of the knee joint in lateral impact: Effect of Shearing Loads, In Proceedings of the IRCOBI 1990, pp. 293-304.
6. Kajzer, J., Cavallero, S., Bonnoit, J., Morjane, A., and Ghanouchi, S., Response of the knee joint in lateral impact: Effect of Bending Moment, In Proceedings of the IRCOBI 1993.

7. Kajzer, J., Schroeder, G., Ishikawa, H., Matsui, Y., and Bosch, U., Shearing and bending effects at the knee joint at high speed lateral loading, In Proceedings of the Society of Automotive Engineers 1997, SAE Paper 973326.

8. Kajzer, J., Ishikawa H., Matsui Y., and Schroeder G., Shearing and bending effects at the knee joint at low speed lateral loading, In Proceedings of the Society of Automotive Engineers 1999, SAE Paper 1999-01-0712.

9. Kerrigan, J., Bhalla, K., Madeley, N., Funk, J., Bose, D., Crandall, J., Experiments for establishing pedestrian impact lower injury criteria, In Proceedings of the Society of Automotive Engineers 2003, SAE Paper 2003-01-0895.

10. K. W. Lia, H. H. Wub and Y. C. Linb, The effect of shoe sole tread groove depth on the friction coefficient with different tread groove widths, floors and contaminants, Applied Ergonomics 37 (2006), pp. 743-748.

11. Maeno, T., and Hasegawa, J., Development of a finite element model of the total human model for safety (THUMS) and application to car-pedestrian impacts, In Proceedings of the 17th ESV conference 2001, Paper No. 494.

12. Mizuno, Y., Summary of IHRA Pedestrian safety WG activities (2003) – proposed test methods to evaluate pedestrian protection afforded by passenger cars, In Proceedings of the 18th ESV conference 2003.

13. Nagasaka, K., Mizuno, K., Tanaka, E., Yamamoto, S., Iwamoto, M., Miki, K., and Kajzer J., Finite element analysis of knee injury in car-to-pedestrian impacts, Traffic Injury Prevention 2003, Vol. 4, pp. 345-354.

14. Schuster, J. P., Chou, C. C., Prasad, P., and Jayaraman, G., Development and validation of a pedestrian lower limb non-linear 3-D finite element model, Stapp Car Crash Journal 2000, Paper No. 2000-01-SC21.

15. Soni, A., Chawla, A., and Mukherjee, S., Effect of muscle contraction on knee loading for a standing pedestrian in lateral impacts, In proceedings of the 20th ESV conference 2007, Paper No. 467.

16. Soni, A., Chawla, A., Mukherjee, S. and Malhotra R., Response of lower extremity in car-pedestrian impact - influence of muscle contraction, In Proceedings of the IRCOBI conference, 2008, pp. 469-472.

17. Takahashi, Y., and Kikuchi, Y., Biofidelity of test devices and validity of injury criteria for evaluating knee injuries to pedestrians, In Proceedings of the 17th ESV conference 2001.

18. Winter, D. A. (1987). Biomechanics & Motor Control of Human Gait, University Waterloo Press.

APPENDIX - A

Values of activation levels used in the present study to model the 42 active muscles in each leg are listed in the Table A.1. These values are taken from Winter (1987). Here, right leg muscles are modeled for 60 % gait (i.e. terminal stance) and left leg muscles are modeled for 0 % gait (i.e. heel strike).

Table A1: Activation levels used in the present study (Note: Activation levels labeled with (*) are taken from Winter (1987))

Lower extremity muscles	Activation levels	
	Left Leg	Right Leg
Vastus Lateralis	0.5*	0.1*
Vastus Intermedius	0.005	0.005
Vastus Medialis	0.005	0.005

Rectus Femoris	0.5*	0.1*
Soleus	0.2*	0.35*
Gastrocnemius Medialis	0.2*	0.2*
Gastrocnemius Lateralis	0.2*	0.3*
Flexor Hallucis Longus	0.005	0.005
Flexor Digitorium Longus	0.005	0.005
Tibialis Posterior	0.005	0.005
Tibialis Anterior	0.4*	0.1*
Extensor Digitorium Longus	0.4*	0.1*
Extensor Hallucis Longus	0.005	0.005
Peroneus Brevis	0.005	0.005
Peroneus Longus	0.4*	0.2*
Peroneus Tertius	0.005	0.005
Biceps Femoris (LH)	0.4*	0.1*
Biceps Femoris (SH)	0.4*	0.1*
Semimembranosus	0.4*	0.1*
Semitendinosus	0.4*	0.1*
Piriformis	0.005	0.005
Pectineus	0.005	0.005
Obturator Internus	0.005	0.005
Obturator Externus	0.005	0.005
Gracilis	0.005	0.005
Adductor Brevis 1	0.005	0.005
Adductor Brevis 2	0.005	0.005
Adductor Longus	0.5*	0.5*
Adductor Magnus 1	0.25*	0.1*
Adductor Magnus 2	0.25*	0.1*
Adductor Magnus 3	0.25*	0.1*
Gluteus Maximus 1	0.5*	0.15*
Gluteus Maximus 2	0.5*	0.15*
Gluteus Maximus 3	0.5*	0.15*
Gluteus Medius 1	0.5*	0.05*
Gluteus Medius 2	0.5*	0.05*
Gluteus Medius 3	0.5*	0.05*
Gluteus Minimus 1	0.005	0.005
Gluteus Minimus 2	0.005	0.005
Gluteus Minimus 3	0.005	0.005
Sartorius	0.4*	0.25*
Tensor Fascia Lata	0.005	0.005